Excited State Properties of Peridinin: Observation of a Solvent Dependence of the Lowest Excited Singlet State Lifetime and Spectral Behavior Unique among Carotenoids

ARTICLE · OCTOBER 1999

DOI: 10.1021/jp9916135

Excited State Properties of Peridinin: Observation of a Solvent Dependence of the Lowest Excited Singlet State Lifetime and Spectral Behavior Unique among Carotenoids

James A. Bautista,[†] Robert E. Connors,[‡] B. Bangar Raju,[†] Roger G. Hiller,[§] Frank P. Sharples,[§] David Gosztola,[||] Michael R. Wasielewski,[||,⊥] and Harry A. Frank*,[†]

Department of Chemistry, University of Connecticut, Storrs, Connecticut 06269-3060, Department of Chemistry and Biochemistry, Worcester Polytechnic Institute, Worcester, Massachusetts 01609, Department of Biological Sciences, Macquarie University, NSW 2109, Australia, Chemistry Division, Argonne National Laboratory, Argonne, Illinois 60439, and Department of Chemistry, Northwestern University, Evanston, Illinois 60208

Received: May 19, 1999

The spectroscopic properties and dynamic behavior of peridinin in several different solvents were studied by steady-state absorption, fluorescence, and transient optical spectroscopy. The lifetime of the lowest excited singlet state of peridinin is found to be strongly dependent on solvent polarity and ranges from 7 ps in the strongly polar solvent trifluoroethanol to 172 ps in the nonpolar solvents cyclohexane and benzene. The lifetimes show no obvious correlation with solvent polarizability, and hydrogen bonding of the solvent molecules to peridinin is not an important factor in determining the dynamic behavior of the lowest excited singlet state. The wavelengths of emission maxima, the quantum yields of fluorescence, and the transient absorption spectra are also affected by the solvent environment. A model consistent with the data and supported by preliminary semiempirical calculations invokes the presence of a charge transfer state in the excited state manifold of peridinin to account for the observations. The charge transfer state most probably results from the presence of the lactone ring in the π-electron conjugation of peridinin analogous to previous findings on aminocoumarins and related compounds. The behavior of peridinin reported here is highly unusual for carotenoids, which generally show little dependence of the spectral properties and lifetimes of the lowest excited singlet state on the solvent environment.

Introduction

Peridinin is the highly substituted carotenoid characteristic of the Peridiniales group of dinoflagellates.[1−3] Its structure is shown in Figure 1 and features an unusual C_{37} carbon skeleton rather than the typical C_{40} system present in most carotenoids, an allene moiety and lactone ring in conjugation with the π-electron system of conjugated carbon−carbon double bonds, together with epoxy and acetate substituents on opposite β-rings.[4] Many of the spectroscopic properties associated with the low-lying excited states of peridinin in solution, and the efficiency and dynamics of energy transfer to and from peridinin and chlorophyll (Chl) *a* in the water-soluble peridinin−Chl *a*−protein (PCP) complex from *Amphidinium carterae* have been examined in detail.[5−8] From studies on peridinin and other carotenoids in solution, it is known that there are at least two important low-lying excited singlet states, denoted S_1 and S_2, that can account for many of the photochemical properties of these molecules. Electronic transitions to and from S_1 and the ground state, denoted S_0, are generally considered to be forbidden by symmetry because both S_0 and S_1 are characterized by an A_g irreducible representation in the idealized C_{2h} point group. In contrast, electronic transitions to and from the S_2 state and the ground state, S_0, are allowed because S_2 possesses B_u symmetry in the same point group. The strong absorption in the visible region characteristic of all polyenes and carotenoids is attributable to the allowed $S_0 \rightarrow S_2$ ($1^1A_g \rightarrow 1^1B_u$) transition.

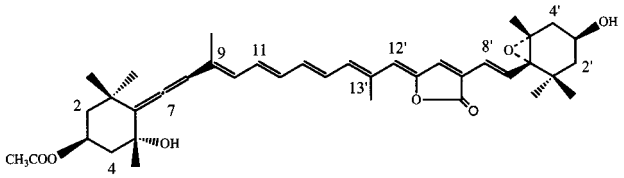

Figure 1. Molecular structure of peridinin.

In several studies on carotenoids and polyenes,[9−12] the energy of the $S_0 \rightarrow S_2$ transition has been shown to vary with solvent polarizability, an effect attributed to dispersion interactions between the strong transition dipole and the solvent environment. The energy of the $S_1 \rightarrow S_0$ transition, however, is hardly affected by solvent due to the fact that its low oscillator strength does not give rise to a significant transition dipole that can be influenced by interactions with the solvent environment.[13] At first glance, peridinin appears to conform to this standard behavior. Peridinin has a strong absorption band in the visible spectrum which shifts to the red with increasing solvent polarizability (see Figure 2 and below), and its fluorescence spectrum is significantly Stokes-shifted indicating that the primary emission from peridinin is from S_1.[6] This is typical of carotenoids and polyenes having fewer than nine carbon−carbon double bonds.[14] On closer inspection, however, peridinin, unlike other carotenoids, displays a pronounced solvent dependence of its lowest excited singlet state lifetime. Akimoto et al.[15] have

* To whom correspondence should be addressed. E-mail: frank@uconnvm.uconn.edu.
[†] University of Connecticut.
[‡] Worcester Polytechnic Institute.
[§] Macquarie University.
[||] Argonne National Laboratory.
[⊥] Northwestern University.

10.1021/jp9916135 CCC: $18.00
Published on Web 09/23/1999

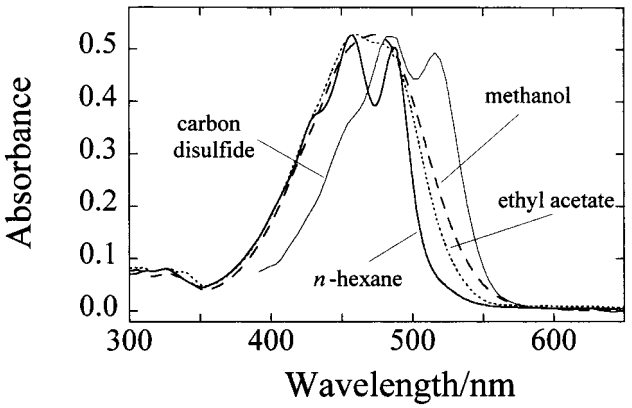

Figure 2. Absorption spectra of peridinin at room temperature in the solvents carbon disulfide, *n*-hexane, methanol, and ethyl acetate. The spectra are representative of the resolved (*n*-hexane), partially resolved (ethyl acetate), and unresolved (methanol) vibronic structure, and red-shifting (carbon disulfide) with increasing solvent polarizability. The spectra were normalized to the same relative maximum absorbance.

measured a value of 103 ps for the S_1 lifetime of peridinin in carbon disulfide using time-resolved single photon counting fluorescence spectroscopy, whereas our recent studies using time-resolved pump−probe laser spectroscopy on peridinin in methanol gave an S_1 lifetime of 13.4 ± 0.6 ps.[6] This apparent discrepancy prompted the present study, which is aimed at uncovering the origin of the solvent dependence of the lifetime of the lowest excited singlet state of peridinin. The photochemical behavior and spectral properties of peridinin are shown here to be highly atypical of carotenoids in general.

Materials and Methods

Sample Preparation. Peridinin was extracted from the PCP complex as previously described[6] and purified by high-performance liquid chromatography (HPLC) using a Millipore Waters 600 E HPLC, a Nova-Pak C18 column and a two-solvent gradient. Solvent A was 50% water/50% solvent B. Solvent B was 50% methanol/50% acetonitrile. The column was equilibrated at a flow rate of 1 mL/min with 80% A for ∼30 min before injection of the sample. Five minutes after injection of the sample, a gradient to 90% B was applied over a period of 10 min, followed by a gradient to 99% B over a period of 5 min, after which time the mobile phase was held at 99% B. The eluent was monitored using the Model 996 single diode array detector, and the fractions containing peridinin were collected and dried using a gentle stream of gaseous nitrogen.

Solvents. The solvents used were *n*-hexane (>99%), benzonitrile (99.9%), cyclohexane (>99.9%), carbon disulfide (99.9%), 1-propanol (99.7%), diethyl ether (99.9%), benzyl alcohol (99.8%), and 2,2,2-trifluoroethanol (99.5%) from Aldrich; di-*n*-propyl ether (>99.5%) and 1,2,4-trichlorobenzene (>99%) from Fluka; ethyl acetate (99.9%), tetrahydrofuran (99.9%), acetone (99.6%), acetonitrile (99.9%), *n*-heptane (99%), and methanol (99.9%) from Fisher; benzene (99.9%), 2-propanol (100.0%), and pyridine (100%) from Baker; and ethanol (100%) from AAPER.

Spectroscopic Methods. *Steady-State Absorption and Fluorescence*. Absorption spectra were recorded at room temperature using a Milton Roy Spectronic 3000 Array photodiode array spectrometer. Fluorescence spectroscopy was also carried out at either room temperature or 12 °C using an SLM Instruments, Inc. Model 8000C spectrofluorimeter employing a 450 W ozone-free xenon arc lamp and a monochromator with a grating having 1500 grooves per mm for excitation. The sample emission passed through a 450 nm cutoff filter, and into another monochromator positioned 90° to the excitation beam. For fluorescence excitation spectroscopy the spectral profile of the incident light was monitored using Rhodamine 610 as a quantum counter. The emission and incident light were detected by two independent Hamamatsu Model R-928 photomultiplier tubes. Contributions resulting from Raman scattering bands of the solvent were removed from the spectra by subtracting a solvent blank taken under identical conditions. Fluorescence spectra were also corrected for the wavelength dependences of the optical components using a correction factor generated by a Spectral Irradiance 45 W quartz-halogen tungsten coiled filament lamp standard.

Time-Resolved Optical Spectroscopy. The transient absorption apparatus used to measure the excited state lifetimes consisted of a homemade, self-mode-locked, Ti:sapphire oscillator that was pumped by the 3 W output from a Spectra Physics Millennia CW frequency-doubled, diode-pumped Nd:YAG laser.[16] The Ti:sapphire oscillator emits 25 fs, 840 nm pulses which were temporally stretched using a double-passed grating/mirror combination to a duration of ca. 200 ps. Chirped pulses were amplified with a homemade Ti:sapphire regenerative amplifier that employed a folded cavity and used a double-step Pockel cell (Medox)/thin film polarizer combination for injection and cavity dumping. The regenerative amplifier was pumped by an intracavity frequency-doubled, Q-switched, Nd:YAG laser (Spectra Physics 3450) that produced 3.8 mJ, 50 ns, 532 nm pulses at a 1.27 kHz repetition rate. The output of the Ti:sapphire regenerative amplifier was recompressed with 70% efficiency using a grating pair to give 200 mJ, 140 fs, 840 nm pulses at a 1.27 kHz repetition rate. Using appropriate beam splitters, about 10 mJ of 840 nm light was used to generate a very smooth white light continuum by focusing it with a 5 cm lens into a 2 mm thick sapphire window. Shot-to-shot intensity fluctuations of the probe beam were generally less than 5%. The remaining 840 nm was frequency doubled with 35% efficiency by using a 2 mm long type I LBO crystal to yield 140 fs, 420 nm pulses.

The 420 nm light was used to pump a two-stage optical parametric amplifier[17] that furnished 140 fs transform limited pulses that were tunable from 470 to 820 nm with energies up to 5 mJ per pulse. Energy of the excitation light on the sample was controlled using a polarizer−$\lambda/2$ waveplate combination. Typically 0.3−1 mJ was used to excite the molecules. The excitation beam was synchronously chopped at half the laser repetition rate. The white light probe beam was split into measuring and reference beams. Arrival of the pump beam relative to the measuring probe beam was accomplished with an optical delay line that used a linear stepping motor (Compumotor) with 1 mm (6.6 fs) resolution. Nearly collinear and codirectional excitation and measuring probe beams were focused into the sample to a 0.3 mm diameter spot size. The carotenoid was dissolved in the solvent and placed in a 2 mm path length cuvette. The wavelength of the measuring and reference probe beams were selected with a computer-controlled monochromator (ISA/SPEX M270). Changes in the transmission of the measuring probe light through the sample and changes in the reference probe beam were monitored by photodiodes. Output of each photodiode was integrated by a gated integrator (Evans), and both signals were digitized and recorded by a personal computer (Gateway P6-200). Data acquisition software monitored the quality of each shot and only averaged shots within 5% of the average intensity of the reference probe beam

level. Kinetic parameters were obtained by iterative reconvolution using the Levenberg−Marquardt algorithm. The instrumental time response was 140 fs at 420 nm.

Computational Methods. A fully optimized structure of peridinin was computed with the AM1 Hamiltonian[18] using the standard minimization techniques of the MOPAC93 program.[19] Exploratory single point INDO/S calculations[20] with configuration interaction (CI) (30 single and 172 double excitations) were performed to investigate the differences in the excited state electronic configurations between untwisted and twisted peridinin. To accommodate size limitations of the INDO/S program, the AM1 geometry was truncated to contain only the conjugated π-electron portion of the carotenoid, as it is assumed that this portion of the molecule gives rise to the low-lying electronic states of peridinin. The truncated AM1 optimized ground-state structure was rotated 90° about the 12′−13′ C−C single bond near the lactone ring (see Figure 1 and discussion below).

Results

Absorption and Fluorescence Spectra. Room temperature absorption spectra of peridinin in *n*-hexane, carbon disulfide, ethyl acetate, and methanol, which are representative of their spectra in increasingly polar solvents, are shown in Figure 2. The spectra are characterized by an intense, broad (fwhm ∼ 4,100−4,800 cm^{-1}) band in the 350−550 nm region which is thought to be associated with the $S_0 \rightarrow S_2$ transition. In nonpolar solvents such as *n*-hexane (Figure 2), the peridinin absorption band has resolved vibronic structure, the longest wavelength feature of which corresponds to the spectral origin which in *n*-hexane is located at 486 nm. Vibronic structure observed for peridinin in nonpolar solvents decreases and ultimately disappears in highly polar or hydrogen bonding solvents such as methanol (Figure 2) or acetonitrile. Also, the width of the absorption band increases asymmetrically as the polarity of the solvent is increased (Figure 2). If a polar solvent is removed by evaporation and the peridinin sample redissolved in a nonpolar solvent, the vibronic structure in the absorption spectrum is fully restored.

A plot of the wavenumber of maximum absorbance for peridinin as a function of solvent polarizability, $R(n) = (n^2 - 1)/(n^2 + 2)$, where *n* is the index of refraction of the solvent, is given in Figure 3. If only the resolved spectra from peridinin in nonpolar solvents (circles in Figure 3) are considered, the plot reveals shifts in the absorption maximum that depend linearly on $R(n)$ as has been observed for many other carotenoids.[9−12] Theoretical models describing the solvatochromic effect on the absorption spectra of nonpolar molecules in nonpolar solvents have described this linear relationship in detail.[12] In polar or hydrogen bonding solvents the description is more complex.[12] For peridinin, the maxima of the absorption spectra in these solvents are at different wavelengths than in the nonpolar solvents, and the shifts do not correlate in a simple linear manner with solvent polarizability (triangles and squares in Figure 3).

A fluorescence spectrum of peridinin taken at room temperature in carbon disulfide at 12 °C is shown in Figure 4. The spectrum is broad and substantially red-shifted relative to the peridinin absorption. The large Stokes shift between the emission (Figure 4) and absorption (Figures 2 and 4) profiles suggests that the fluorescence emission from peridinin corresponds to an $S_1 \rightarrow S_0$ ($2^1A_g \rightarrow 1^1A_g$) transition rather than an $S_2 \rightarrow S_0$ ($1^1B_u \rightarrow 1^1A_g$) transition.[6] The positions of the emission maxima for peridinin in several solvents are given in Table 1 and

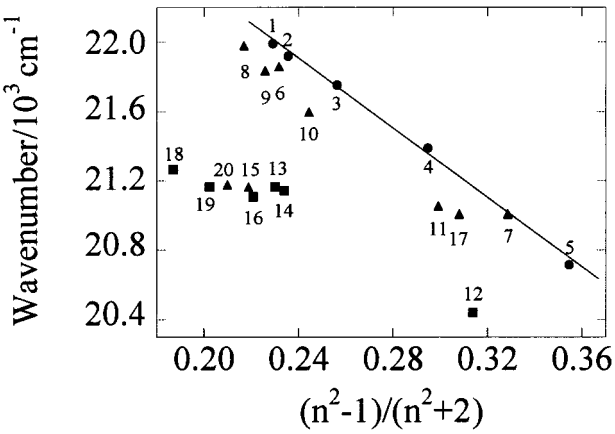

Figure 3. Plot of the wavenumber of maximum absorbance of the $S_0 \rightarrow S_2$ transition for peridinin as a function of the solvent polarizability factor, $R(n) = (n^2 - 1)/(n^2 + 2)$, where n is the index of refraction of the solvent. The circles (●), triangles (▲), and squares (■) represent peridinin in nonpolar, polar, and hydrogen bonding solvents, respectively. The error in the points is approximately ±100 cm^{-1} and is derived from the uncertainty in assigning the wavelengths of maximum absorption. The data points and solvent key are given in Table 2.

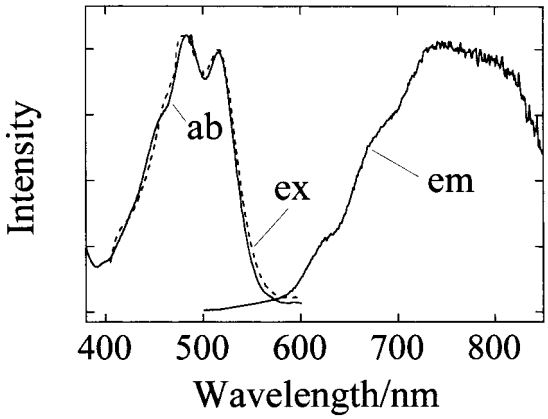

Figure 4. Absorbance, fluorescence, and fluorescence excitation spectra of peridinin in carbon disulfide. The absorption was taken at room temperature. The fluorescence and fluorescence excitation spectra were taken at 12 °C. The vertical scale is arbitrary. The spectra were all normalized to their peak maxima. The spectra were taken using the following experimental conditions: excitation wavelength, 456 nm; slit, 16 nm; integration time, 1 s; scan rate, 0.95 nm/s.

represent the range of wavelengths spanned by the emission in the nonpolar and polar solvents. In general, the emission maxima lie more to the red in the polar solvents than in the nonpolar solvents.

The intensity of the peridinin emission is also strongly solvent dependent. The emission is strongest in the nonpolar solvent, carbon disulfide, and weakest in the more polar or hydrogen bonding solvents, such as methanol or acetonitrile. The quantum yields of peridinin emission in various solvents were determined by integrating the emission profiles such as that given in Figure 4, and then comparing the results with the integrated emission obtained from a Rhodamine 800 standard which has a quantum yield of 0.086 in methanol.[21] The resulting values for the quantum yields of peridinin are given in Table 1.

Transient Absorption Experiments. Excitation of peridinin into its strong absorption band with a laser pump results in a rapid buildup of a transient absorption which was probed using a white light continuum. The transient absorption decays rapidly with single-exponential kinetics to zero as the excited singlet state is depopulated primarily by internal conversion to the

TABLE 1: Fluorescence Quantum Yields, Φ_f, Wavelengths of Emission Maxima, λ^e_{max}, Solvent Polarity Factors, $P(\epsilon)$, Radiative Rate Constants, k_{rad}, and Nonradiative Rate Constants, k_{nrad}, of the S_1 State of Peridinin in Various Solvents[a]

solvent	Φ_f	λ^e_{max}/nm	$P(\epsilon)$	k_{rad}/s^{-1}	k_{nrad}/s^{-1}
carbon disulfide	3.6×10^{-3}	737	0.354	2.1×10^7	6.0×10^9
ethyl acetate	1.4×10^{-3}	749	0.626	n.d.	n.d.
n-hexane	8.7×10^{-4}	715	0.229	6.1×10^6	6.2×10^9
methanol	1.2×10^{-4}	721	0.913	n.d.	n.d.
acetonitrile	5.8×10^{-5}	781	0.921	n.d.	n.d.

[a] The Φ_f values were determined by integrating the fluorescence emission profiles on a wavenumber scale after bandpass correction and then comparing the results with the integrated emission obtained from a Rhodamine 800 standard. The polarity factors were determined from the dielectric constants for the solvents using the expression $P(\epsilon) = (\epsilon - 1)/(\epsilon + 2)$. The k_{rad} values were calculated by dividing the quantum yields of fluorescence by the lifetimes, τ, of the excited state given in Table 2. The k_{nrad} values were determined from the measured lifetimes and the k_{rad} values using the expression $\tau = 1/(k_{rad} + k_{nrad})$. The Φ_f values have a relative error of approximately 10% and an absolute error of approximately 30% derived primarily from the uncertainty in the integration of the fluorescence band shapes. The errors in the k_{rad} and k_{nrad} values are propagated to be approximately 32%. The error in the λ^e_{max} values is ±3 nm and derives from experimental uncertainty owing to limitations in signal-to-noise ratio of the fluorescence measurements and in the broadness of the spectral traces. n.d. means not determined because obtaining k_{rad} and k_{nrad} values from the emission quantum yields and lifetimes of the excited state is only strictly valid if the emission and dynamics originate from the same state. For peridinin in the polar solvents this is not likely to be the case.

ground state. Representative decay traces for peridinin in increasingly polar solvents are shown in Figure 5. As can be seen from the figure and Table 2, the lifetime of the lowest excited singlet state of peridinin is highly solvent dependent. The lifetime is shortest (<10 ps) in the highly polar solvent, acetonitrile, and in the strongly hydrogen bonding solvent, trifluoroethanol, and longest (~165 ps) in nonpolar solvents such as carbon disulfide and *n*-hexane. In virtually all cases, the values of the lifetimes did not depend on the wavelength of the probe beam from 513 to 710 nm. A plot of the lifetime of the lowest excited singlet state versus the solvent polarity function, $P(\epsilon)$, is given in Figure 6. The lifetime is constant to a point where $P(\epsilon) \sim 0.4$, but at polarity values larger than 0.4, the lifetime decreases linearly with increasing solvent polarity (Figure 6).

Representative transient absorption spectra of peridinin in increasingly polar solvents are shown in Figure 7. At least two bands are evident in the spectra from peridinin in *n*-hexane, ethyl acetate, and 2-propanol. The first band appears at ~510 nm in *n*-hexane and red-shifts slightly as the solvent polarity is increased. Although the wavelength of this band is not strongly affected by the solvent environment, its intensity diminishes significantly as the polarity of the solvent is increased (Figure 7). In strongly polar or hydrogen bonding solvents such as methanol, the band is barely noticeable as a small shoulder on the short wavelength side of the transient spectrum (Figure 7). The second band in the transient spectra is at ~660 nm in the nonpolar solvent, *n*-hexane, and shifts significantly to shorter wavelength as the solvent polarity is increased, appearing at ~590 nm in methanol (Figure 7).

Discussion

The strong solvent dependence of the spectral properties and dynamics associated with the lowest excited singlet state of peridinin is highly unusual among carotenoids. Typically, the extremely low oscillator strength of the $S_0 \rightarrow S_1$ transition of carotenoids and polyenes is related to a vanishingly small transition dipole moment that is hardly affected by the solvent environment.[13] This is in contrast to the large transition dipole associated with the $S_0 \rightarrow S_2$ absorption of these molecules, which is strongly affected by dispersion interactions with the solvent environment, and is the major source of spectral shifts observed for carotenoids in solution.[9−12] Upon dissolving a carotenoid or polyene, the typically observed behavior is a shift in the absorption spectrum that depends linearly on the polarizability of the solvent.[10,13,22]

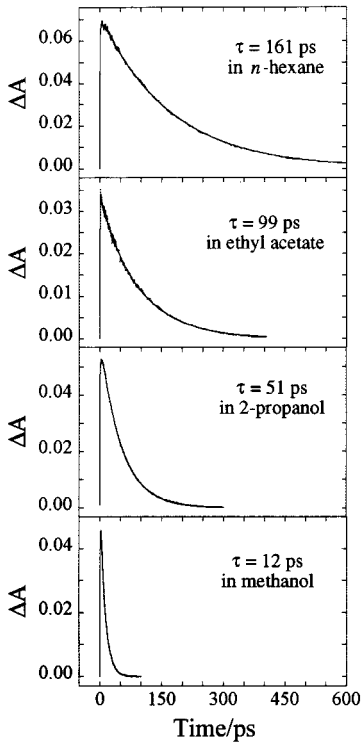

Figure 5. Representative fast transient decay traces for peridinin in increasingly polar solvents. Excitation was accomplished by exciting peridinin into its strong absorption band with a laser pump and probing the transient absorption using a white light continuum tuned to a specific probe wavelength in the transient absorption spectrum. The transient absorptions decay in virtually all cases with single-exponential kinetics that do not depend on the probe wavelength from 513 to 710 nm. The excited singlet state lifetimes for peridinin are derived from these measurements and are given for these and several other solvents in Table 2.

For peridinin in polar solvents, the lifetime of the lowest excited singlet state did not correlate with the polarizability of the solvent, but instead was linearly dependent on the polarity of the solvent (Figure 6). With solvents of increasing dielectric strength, the $S_0 \rightarrow S_2$ absorption became broader and less structured (Figure 2), and the lifetime of the lowest excited singlet state became shorter (Table 2). The origin of the effect of different solvents on the spectroscopic properties of peridinin may be attributable to the fact that it is highly substituted compared to most other carotenoids. Peridinin has an allene moiety and a lactone ring, both of which are connected directly to its π-electron conjugated system (Figure 1). The presence of a carbonyl group in the conjugated chain has also been shown to affect the origin of fluorescence.[23] Neoxanthin, which lacks the lactone ring and its associated carbonyl, but otherwise is similar in structure to peridinin, fluoresces predominantly from the S_2 state, whereas peridinin is an S_1 emitter.[23] The dependence of the spectral properties of these molecules on the presence of a carbonyl suggests that the coupling of nπ* states derived from

TABLE 2: The Lifetimes, τ, Solvent Polarizability Factors, $R(n)$, Solvent Polarity Factors, $P(\epsilon)$, Energies of Maximum Absorption for the $S_0 \rightarrow S_2$ Transition, ν_{abs}, and Vibronic Structure Associated with the $S_0 \rightarrow S_2$ Absorption Profile of Peridinin in Various Solvents[a]

solvent	no.	τ/ps	$R(n)$	$P(\epsilon)$	ν_{abs}/cm^{-1}	vibronic structure
n-hexane	1	161	0.229	0.229	21 990	R
n-heptane	2	166	0.235	0.239	21 920	R
cyclohexane	3	172	0.256	0.254	21 750	R
benzene	4	172	0.295	0.300	21 390	R
carbon disulfide	5	168	0.354	0.354	20 720	R
propyl ether	6	166	0.232	0.434	21 860	P
1,2,4-trichlorobenzene	7	145	0.329	0.512	21 000	P
diethyl ether	8	157	0.217	0.526	21 980	P
ethyl acetate	9	99	0.226	0.626	21 830	P
tetrahydrofuran	10	79	0.244	0.687	21 600	P
pyridine	11	14	0.299	0.790	21 050	P
benzyl alcohol	12	35	0.314	0.801	20 440	N
2-propanol	13	51	0.230	0.852	21 160	N
1-propanol	14	43	0.234	0.864	21 140	N
acetone	15	17	0.219	0.868	21 670	N
ethanol	16	27	0.221	0.886	21 110	N
benzonitrile	17	21	0.308	0.890	21 000	N
2,2,2-trifluoroethanol	18	7	0.1870	0.895	21 265	N
methanol	19	12	0.202	0.913	21 160	N
acetonitrile	20	9	0.210	0.921	21 180	N

[a] The table is sorted by increasing solvent polarity factor. The lifetimes were determined by fast-transient spectroscopy as described in the text and have an uncertainty of approximately ±10% for the values at the bottom of the table and approximately ±5% for the numbers at the top of the table based on the reproducibility of the measurements. The τ values reported here were probed in the spectral region between 590 and 710 nm corresponding to the longest wavelength feature of the transient absorption spectrum. No dependence of the dynamics on the probe wavelength was observed between 513 and 710 nm. The solvent polarizability and polarity factors were determined from the dielectric constants and indices of refraction for the solvents using the expressions $P(\epsilon) = (\epsilon - 1)/(\epsilon + 2)$ and $R(n) = (n^2 - 1)/(n^2 + 2)$, respectively. The ν_{abs} values were measured from the absorption spectra and have an error of approximately ±100 cm^{-1} derived from the uncertainty in assigning the wavelengths of maximum absorption. The vibronic structure in the absorption spectra are categorized as being R, for resolved, P, for partially resolved, or N, for none. See Figure 3 for examples.

the functional group to S_1 and S_2 may affect the dynamics of the lowest excited singlet state of peridinin. However, this is inconsistent with the data presented here.

The major effect of low-lying nπ* states would be to shorten the lifetime of the lowest lying excited singlet state by enhancing the rate of intersystem crossing to the triplet state, because electronic coupling between nπ* states and $\pi\pi$* states in proximity is well-known to increase triplet state yields and reduce singlet state lifetimes.[24] In solvents capable of hydrogen bonding, the effect is however diminished, and hydrogen bonding of a solvent molecule to the carbonyl oxygen of peridinin would be expected to stabilize the occupied n orbital and result in a shift of the nπ* state to higher energy. In this case, the lifetime of the S_1 state of peridinin would be predicted to become longer in hydrogen bonding solvents, rather than shorter as observed here (Table 2). Furthermore, the fact that the lifetime of the lowest excited singlet state of peridinin in the non hydrogen bonding solvent, acetonitrile, is comparable to its lifetime in the hydrogen bonding solvents, trifluoroethanol and methanol, is strong evidence that protonation of the carbonyl oxygen plays no role in the solvent dependence of its lifetime. The carotenoid, fucoxanthin, which has an allene group and a carbonyl in conjugation with the π-electron system, but not the lactone ring, emits predominantly from its S_1 state like peridinin,

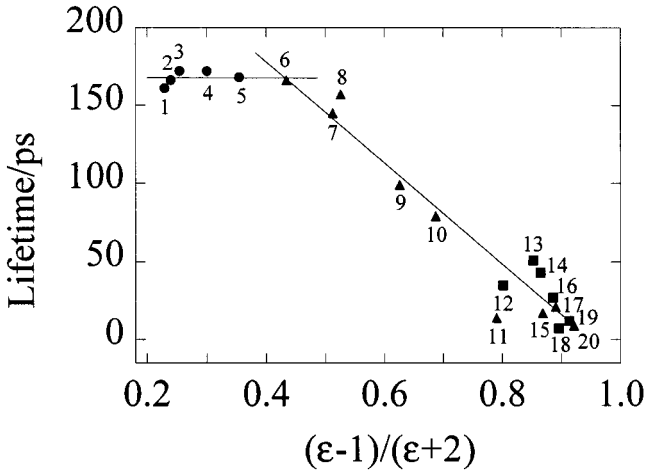

Figure 6. Plot of the lifetime of the lowest excited singlet state of peridinin versus the solvent polarity function, $P(\epsilon) = (\epsilon - 1)/(\epsilon + 2)$. The circles (●), triangles (▲), and squares (■) represent peridinin in nonpolar, polar, and hydrogen bonding solvents, respectively. The lifetime is in the nonpolar solvents (●) to a point where $P(\epsilon) \sim 0.4$. At polarity values larger than 0.4, the lifetime decreases linearly with increasing solvent polarity. The values for the lifetimes and polarity factors are given in Table 2. The uncertainties in the lifetimes are approximately ±10% for the values in the polar solvents and approximately ±5% for the values in the nonpolar solvents based on the reproducibility of the measurements.

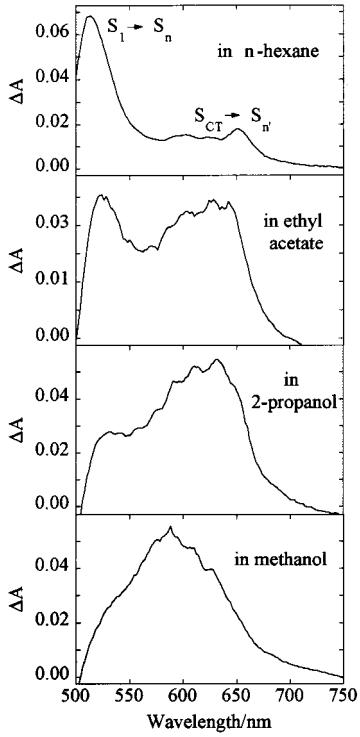

Figure 7. Representative transient absorption spectra of peridinin captured 5 ps after excitation in solvents of increasing polarity. At least two bands are evident in the spectra from peridinin in *n*-hexane, ethyl acetate, and 2-propanol. The first band appears at ~510 nm in *n*-hexane and red-shifts slightly as the solvent polarity is increased. The second band appears at ~660 nm in *n*-hexane and shifts significantly to shorter wavelength as the solvent polarity is increased, appearing at ~590 nm in methanol.

and has been reported to have a 41 ps S_1 lifetime in carbon disulfide[25] and a 40 ps S_1 lifetime in ethanol.[26] This suggests that the lactone ring may be the central feature controlling the effect of solvent on the spectral properties and dynamics of peridinin.

Rechthaler and Köhler[27] have studied the effect of solvent polarity on the photophysical properties of several aminocoumarins which are similar to peridinin in that they are conjugated π-electron systems containing a lactone ring. In nonpolar solvents the absorption band shapes of the aminocoumarins have resolved vibronic structure, whereas in polar, hydrogen bonding solvents the spectra are broad and featureless. In solvents having dielectric constants less than 10, the fluorescence quantum yields of several of the aminocoumarins are very high ($\sim$1), and the lifetime of the excited singlet state is constant at $\sim$ 5 ns. In solvents having dielectric constants greater than 10, quenching of the fluorescence from the aminocoumarins and a reduction in the singlet state lifetime is observed to depend linearly on the polarity function, $P(\epsilon)$. An additional nonradiative deactivation pathway via a twisted intramolecular charge transfer (TICT) state was proposed to account for the observations. This hypothesis was supported by experimental determinations of the excited state dipole moments of the aminocoumarins and by semiempirical computations. TICT states may account for the effects of solvent environment on the fluorescence properties of several π-electron systems containing amines, although the phenomenon of intramolecular charge transfer has also been investigated extensively in bianthryl.[28] Many of these molecules have been used extensively in excited state solvation measurements.[28] Although the dielectric thresholds for the solvent effects are different for peridinin compared to the aminocoumarins, the similarity in behavior is striking.

Because of the similarities in structure and spectroscopic behavior between the aminocoumarins and peridinin, it is tempting to suggest that a TICT state, may in fact, exist for peridinin and account for its unique properties among carotenoids. Preliminary semiempirical computations using single and double excited configurations show that the lowest excited singlet state for the truncated peridinin molecule possessing a 90° twist between carbons 12′ and 13′ (Figure 1) is, in fact, a TICT state corresponding to a HOMO(π-chain) $\rightarrow$ LUMO-(lactone ring) excitation. Assuming the lactone ring is the electron acceptor, the moiety that is expected to be the donor is that with the lowest ionization potential. For this reason the untwisted part of the polyene chain was kept as long as possible since ionization potential decreases with increasing conjugated chain length. For carotenoids, oxidation potentials follow a similar trend.[29] An INDO/S calculation (100 single excitations) has also been carried out on untruncated peridinin with a 90° twist between carbons 12′ and 13′, and a similar TICT state (dipole moment = 31.7 D) has been obtained for the HOMO $\rightarrow$ LUMO excitation. The energy of this gas-phase TICT state is predicted to be higher than the untwisted AM1 optimized structure. These preliminary and exploratory calculations should not be taken to suggest that stabilization of this particular TICT structure in polar solvents is responsible for the effects on the lifetime and quantum yields that have been observed for peridinin. However, the computations do suggest that an explanation involving some charge transfer character in the excited state manifold of peridinin is not unreasonable.

Support for the hypothesis that peridinin possesses a low-lying charge transfer state is obtained by comparing the transient spectra shown in Figure 7 with spectra from similar experiments presented in the literature. Okada et al.[30] have reported transient data from 4-(9-anthryl)-*N*,*N*-dimethylaniline (ADMA) and related compounds which possess TICT states, and found multiple excited states with transient profiles very similar to those observed here. In the spectrum from ADMA and 1-methyl-5-(9-anthryl)indoline (MAI), two bands in the transient spectra were observed. One of the bands is narrow and appears at shorter visible wavelength in nonpolar solvents than the other band. This first band red-shifts only slightly, but decreases markedly in intensity as the polarity of the solvent is increased, and in highly polar solvents such as acetonitrile, is too weak to be observed. The second band in the transient spectra of ADMA or MAI is much broader than the first band and appears at longer visible wavelengths in nonpolar solvents, shifting significantly to shorter wavelengths as the solvent polarity is increased. This second band was assigned to the anion component of a charge transfer state in the molecules. As is evident from this discussion and Figure 7, the transient spectra of ADMA and related compounds and their dependence on solvent are strikingly similar to the spectral behavior seen here for peridinin.

As mentioned above, in solvents having a low dielectric constant, the quantum yield of fluorescence from peridinin is relatively high, and in solvents having a high dielectric constant, the quantum yield is relatively low (Table 1). The radiative rate constants, k_{rad}, for the decay of the emission from peridinin in the nonpolar solvents, calculated by dividing the quantum yields of fluorescence by the lifetimes of the excited states (Table 1), are $\sim 1 \times 10^7$ s^{-1} and typical of carotenoid and polyenes in general. The reduction in the quantum yields of emission in the polar solvents can be understood by considering the rate constant associated with the nonradiative decay (k_{nrad}) from its excited singlet state. The nonradiative pathways possible for peridinin are $S_1 \rightarrow S_0$ internal conversion and intersystem crossing to the triplet state. For carotenoids the efficiency of intersystem crossing from the singlet state to a low-lying triplet state is, in general, very small[31] and hence, any effect on k_{nrad} due to an increase in intersystem crossing can be discounted. This suggests that an additional route for radiationless deactivation of peridinin from its excited S_1 state has become available in polar solvents. It is important, however, to explore whether a simple change in the energy of the emitting state of peridinin, brought about by dissolving it in different solvents, would be sufficient to account for the range of lifetimes from $\sim$165 ps in nonpolar solvents to 7 ps in acetonitrile.

The shift in the emission maxima with solvent environment is represented by the data in Table 1 indicating that an energy range of $\sim$1100 cm^{-1} is spanned by peridinin in the different solvents. This is too small to account for the factor of $\sim$24 difference in lifetime.[32−34] To obtain more than an order of magnitude alteration in the dynamics as is observed here, an energy change of at least $\sim$3000 cm^{-1} for S_1 would be required. Thus, it is unlikely that the different lifetimes of the lowest excited singlet state of peridinin in the various solvents are explained solely on the basis of a mechanism that simply changes the energy of the S_1 state. Also, the changes in the peridinin lifetime do not depend on the position of the S_2 state relative to S_1. This is supported by the observation that peridinin in carbon disulfide and *n*-hexane exhibit essentially the same excited state lifetime despite the fact that, based on the spectral origins of absorption and emission, the change in the S_2-S_1 energy gap for peridinin in carbon disulfide versus *n*-hexane is $\sim$750 cm^{-1}. Nonradiative relaxation involving a nonemissive charge transfer state that quenches fluorescence emission from S_1 is the most likely reason for the large effect of solvent polarity on the dynamics of the excited singlet state. The charge transfer state could be a TICT state, as suggested by the literature on aminocoumarins, ADMA, and other related compounds, and supported by the exploratory INDO/S computations described

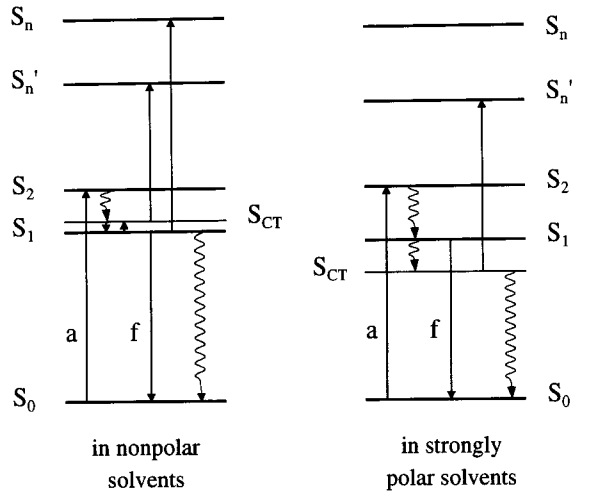

Figure 8. Energy state diagram depicting the photochemical behavior of peridinin dissolved in solvent in the limits of nonpolar and strongly polar character. The strongly allowed $S_0 \rightarrow S_2$ absorption is labeled with the letter "a". $S_1 \rightarrow S_0$ fluorescence is labeled with the letter "f". Excited singlet states S_n and $S_{n'}$ are shown into which transient absorption (vertical arrows) may occur. A charge transfer state, S_{CT}, in the excited state manifold of peridinin is shown to be higher in energy than the S_1 state in nonpolar solvents and shifts below S_1 with increasing solvent polarity. In the nonpolar solvent case, two transient absorptions are observed, and in the strongly polar solvent case only one transition is observed. In nonpolar solvents, S_{CT} is sufficiently close in energy to S_1 that it may be thermally populated after light absorption, a, and fast internal conversion (wavy lines). In strongly polar solvents the S_1 state of peridinin and its associated fluorescence is quenched by the low-lying S_{CT} state.

above, or a nontwisted intramolecular charge transfer (ICT) state both of whose energies are known to be highly susceptible to solvent environment.[35]

An energy state diagram that could explain the behavior of peridinin in the various solvents is given in Figure 8. The figure depicts a hypothetical energy scheme for peridinin dissolved in solvents of low and high polarity. From the striking similarity between the spectral behavior of peridinin compared to the aminocoumarins, ADMA, and other related compounds, where charge transfer states are clearly evident,[30] an additional state in the excited state manifold of peridinin is justified and assigned to a nonemissive charge transfer state, denoted S_{CT} in Figure 8. In nonpolar solvents, S_{CT} would be higher in energy than the S_1 state, yet sufficiently close in energy to S_1 that it may be thermally populated after light absorption and fast internal conversion from S_2 to either S_{CT} or S_1. This would account for the observation of two electronic transitions in the transient spectral profiles from peridinin in low dielectric media (Figure 7). The shorter-wavelength, narrow band is observed in all known transient spectra from carotenoids and can be assigned to an $S_1 \rightarrow S_n$ transition. (e.g., see ref 36). The longer-wavelength, broader transition can be assigned to the $S_{CT} \rightarrow S_{n'}$ component of the spectra because of its marked similarity with that from ADMA and other related compounds which are attributable to such transitions.[30] Also, in solvents having low dielectric strengths, the singlet state lifetime remains essentially constant at ~165 ps (Figure 6), because it is determined primarily by the decay of S_1 directly to the ground state. In solvents having a dielectric constant greater than 3 (polarity factor > 0.4), the observed lifetime decreases linearly with the polarity function, $P(\epsilon)$ (see Figure 6), because in this region the charge transfer state, S_{CT}, has dropped below S_1, enhancing the probability of depopulation.

A model involving a charge transfer state in the peridinin excited state manifold is also consistent with the observations of a significant reduction in intensity of the high-energy $S_1 \rightarrow S_n$ band and a substantial blue-shift in the low-energy $S_{CT} \rightarrow S_{n'}$ band with increasing solvent polarity analogous to that observed by Okada et al.[30] for ADMA and related compounds. For peridinin in increasingly polar solvents, the population in S_1 is more efficiently depleted by the S_{CT} state dropping below S_1, thereby reducing the intensity of the $S_1 \rightarrow S_n$ band. The low-energy $S_{CT} \rightarrow S_{n'}$ band in the transient absorption spectrum of peridinin is strongly solvent dependent because it represents absorption from the charge transfer state itself to a higher excited singlet state. Owing to the strong dipolar nature of the charge transfer state, its energy is expected to change with variations in the polarity of the solvent environment.

The model depicted in Figure 8 would predict a reduction in the quantum yield of fluorescence from peridinin with increasing solvent polarity as is observed. It is known that low-lying charge transfer states can quench fluorescence by enhancing nonradiative deactivation.[37] It is perhaps surprising, however, that the fluorescence is not fully quenched in the very polar solvents. It is also surprising that the $S_1 \rightarrow S_n$ and $S_{CT} \rightarrow S_{n'}$ transient absorptions decay with essentially the same single-exponential kinetics in all of the cases where both transitions can be observed. The model presented in Figure 8 accounts for this by invoking a small energy gap and strong thermal coupling between the S_1 and S_{CT} states for peridinin in the nonpolar solvents. Measurements of the temperature dependence of the kinetics of the $S_1 \rightarrow S_n$ and $S_{CT} \rightarrow S_{n'}$ transient absorptions and their rise dynamics would be useful in testing the model presented here which presents the most plausible, albeit hypothetical, interpretation for the current experimental observations.

Peridinin in the PCP complex is characterized by a strong, unresolved, visible absorption band, a single, broad, unstructured transient absorption feature, and an energy transfer efficiency to Chl of 88 ± 2% measured by steady state fluorescence excitation spectroscopy.[6] These properties are consistent with peridinin in the PCP complex residing in a highly polar electrostatic environment in the protein. Indeed, the three-dimensional structure of the protein from *Amphidinium carterae*[8] reveals polar hydrogen bonding residues in close proximity to the lactone rings of the bound peridinins (E. Hoffman, private communication).

Is there a physiological role for a low-lying charge transfer state of peridinin in vivo? Could S_{CT} be an energy donor to Chl? The position of the S_{CT} state near S_1, its strong susceptibility to the solvent environment, and its ability to influence the dynamics of the S_1 state suggest that it may play a role in regulating flow of energy to Chl. When photosynthetic organisms are exposed to high light intensities, they are prone to photoinhibition unless photoprotective mechanisms are activated.[38] Quenching of the S_1 excited state of peridinin by a low-lying charge transfer state may provide a mechanism by which energy in excess of that required to carry out photosynthesis could be diverted from the reaction center. In the case of an organism containing peridinin, the extent of quenching could be modulated with modifications to the protein environment in the vicinity of the carotenoid. Further investigations will be required to confirm if peridinin in either PCP or the intrinsic light-harvesting complex is capable of regulating photosynthetic energy flow. Nevertheless, the unique properties of this carotenoid make it a good candidate for this role.

Acknowledgment. The authors thank Professors Robert Birge, Ron Christensen, and Klaus Schulten for useful discussions. We also thank Jesusa Josue for help with the fluorescence experiments. This work was supported by grants to H.A.F. from the National Institutes of Health (GM-30353), the National Science Foundation (MCB-9816759), and the University of Connecticut Research Foundation. R.E.C. thanks Worcester Polytechnic Institute for a sabbatical leave. He also appreciates the hospitality extended to him by the University of Connecticut during his leave. The work at Argonne National Laboratory was supported by the Office of Basic Energy Sciences, Division of Chemical Sciences, U.S. Department of Energy, under Contract W-31-109-Eng-38. R.G.H. was supported by Australian Research Council Grant A19600918.

References and Notes

(1) Goodwin, T. W. *The Biochemistry of the Carotenoids*, 2nd ed.; Chapman & Hall: London, 1980; Vol. 1, p 220.

(2) Liaaen-Jensen, S. In *Carotenoids*; Britton, G., Liaaen-Jensen, S., Pfander, H., Eds.; Birkhäuser Verlag: Berlin, 1998; Vol. 3, p 217.

(3) Johansen, J. E.; Svec, W. A.; Liaaen-Jensen, S.; Haxo, F. T. *Phytochemistry* **1974**, *12*, 2261.

(4) Liaaen-Jensen, S. In *Carotenoids*; Isler, O., Gutmann, H., Solms, U., Eds.; Birkhäuser Verlag: Basel, 1971; p 163.

(5) Koka, P.; Song, P. *Biochim. Biophys. Acta* **1977**, *495*, 220.

(6) Bautista, J. A.; Hiller, R. G.; Sharples, F. P.; Gosztola, D.; Wasielewski, M.; Frank, H. A. *J. Phys. Chem. A* **1999**, *103*, 2267.

(7) Song, P.; Koka, P.; Prezelin, B.; Haxo, F. *Biochemistry* **1976**, *15*, 4422.

(8) Hofmann, E.; Wrench, P.; Sharples, F. P.; Hiller, R. G.; Welte, W.; Diedrichs, K. *Science* **1996**, *272*, 1788.

(9) Le Rosen, A. L.; Reid, C. E. *J. Chem. Phys.* **1952**, *20*, 233.

(10) Andersson, P. O.; Gillbro, T.; Ferguson, L.; Cogdell R. *J. Photochem. Photobiol.* **1991**, *54*, 353.

(11) Nagae, H.; Kuki, M.; Cogdell, R. J.; Koyama, Y. *J. Chem. Phys.* **1994**, *101*, 6750.

(12) Basu, S. *Adv. Quantum Chem.* **1964**, *1*, 145.

(13) Hudson, B. S.; Kohler, B. E.; Schulten, K. In *Excited States*; Lim, E. C., Ed.; Academic Press: New York, 1982; Vol. 6, pp 1−95.

(14) DeCoster, B.; Christensen, R. L.; Gebhard, R.; Lugtenburg, J.; Farhoosh, R.; Frank, H. A. *Biochim. Biophys. Acta* **1992**, *1102*, 107.

(15) Akimoto, S.; Takaichi, S.; Ogata, T.; Nishimura, Y.; Yamazaki, I.; Mimuro, M. *Chem. Phys. Lett.* **1996**, *260*, 147.

(16) Gosztola, D.; Yamada, H.; Wasielewski, M. R. *J. Am. Chem. Soc.* **1995**, *117*, 2041.

(17) Greenfield, S. R.; Wasielewski, M. R. *Opt. Lett.* **1995**, *20*, 1394.

(18) Dewar, M. J. S.; Zoebisch, E. G.; Healy, E. F.; Stewart, J. J. P. *J. Am. Chem. Soc.* **1985**, *107*, 3902.

(19) Stewart, J. J. P. *MOPAC93*; Fujitsu Ltd., 1993.

(20) Ridley, J.; Zerner, M. *Theor. Chim. Acta* **1973**, *32*, 111.

(21) Benfey, D. B.; Brown, D. C.; Davis, S. J.; Piper, L. G.; Foutter, R. F. *Appl. Opt.* **1992**, *31*, 7034.

(22) Hudson, B. S.; Kohler, B. E. *Annu. Rev. Phys. Chem.* **1974**, *25*, 437.

(23) Mimuro, M.; Nagashima, U.; Takaichi, S.; Nishimura, Y.; Yamazaka, I.; Katoh, T. *Biochim. Biophys. Acta* **1992**, *1098*, 271.

(24) Lim, E. C.; Yu, J. M. H. *J. Chem. Phys.* **1967**, *47*, 3270.

(25) Katoh, T.; Nagashima, U.; Mimuro, M. *Photosynth. Res.* **1991**, *27*, 221.

(26) Shreve, A. P.; Trautman, J. K.; Owens, T. G.; Albrecht, A. C. *Chem. Phys.* **1991**, *154*, 171.

(27) Rechthaler, K.; Köhler, G. *Chem. Phys.* **1994**, *189*, 99.

(28) Barbara, P. F.; Jarzeba, W. In *Advances in Photochemistry*; Volman, D. H., Hammond, G. S., Gollnick, K., Eds.; Wiley-Interscience: New York, 1990; Vol. 15, pp 1−68.

(29) Broszeit, G.; Diepenbrock, F.; Gräf, O.; Hecht, D.; Heinze, J.; Martin, H.-D.; Mayer, B.; Schaper, K.; Smie, A.; Strehblow, H.-H. *Liebigs Ann./Recl.* **1997**, 2205.

(30) Okada, T.; Mataga, N.; Baumann, W.; Siemiarczuk. A. *J. Phys. Chem.* **1987**, *91*, 4490.

(31) Frank, H. A.; Bolt, J. D.; De B. Costa, S. M.; Sauer, K. *J. Am. Chem. Soc.* **1980**, *102*, 4893.

(32) Frank, H. A.; Desamero, R. Z. B.; Chynwat, V.; Gebhard, R.; van der Hoef, I.; Jansen, F. J.; Lugtenburg, J.; Gosztola, D.; Wasielewski, M. R. *J. Phys. Chem.* **1997**, *101*, 149.

(33) Desamero, R. Z. B.; Chynwat, V.; van der Hoef, I.; Jansen, F. J.; Lugtenburg, J.; Gosztola, D.; Wasielewski, M. R.; Cua, A.; Bocian, D. F.; Frank, H. A. *J. Phys. Chem.* **1938**, *42*, 8151.

(34) Chynwat, V.; Frank, H. A. *Chem. Phys.* **1995**, *194*, 237.

(35) Rettig, W. *Angew. Chem., Int. Ed. Engl.* **1986**, *25*, 971.

(36) Frank, H. A.; Cua, A.; Chynwat, V.; Young, A.; Gosztola, D.; Wasielewski, M. R. *Photosynth. Res.* **1994**, *41*, 389.

(37) Moore, R. A.; Lee, J.; Robinson, G. W. *J. Phys. Chem.* **1985**, *89*, 3648.

(38) Andersson, B.; Aro, E.-M. *Physiol. Plant.* **1997**, *100*, 780.